Journal of Environmental Management 355 (2024) 120442

Contents lists available at ScienceDirect

Journal of Environmental Management

journal homepage: www.elsevier.com/locate/jenvman

Research article

Using numerical methods for map the spatiotemporal geogenic and anthropogenic influences on the groundwater in a detrital aquifer in south Spain

Juan Antonio Luque-Espinar [a,*], Manuel López-Chicano [b], Eulogio Pardo-Igúzquiza [c], Mario Chica-Olmo [b]

[a] Geological and Mining Institute of Spain from the National Research Council (CSIC-IGME), Urb Alcázar del Genil, edf Zulema 4 bajo, 18006, Granada, Spain
[b] Department of Geodynamics, University of Granada, Av. Fuentenueva s/n, 18071, Granada, Spain
[c] Instituto de Geociencias (CSIC-UCM), c/ Severo Ochoa, 7, 28040, Madrid, Spain

ARTICLE INFO

Handling Editor: Raf Dewil

Keywords:
Trace elements
Groundwater quality
Anthropogenic activity
Geostatistical data analysis

ABSTRACT

The presence of trace elements in water for domestic supply or irrigation could pose a significant toxic risk for health, due to direct consumption or bioaccumulation through the ingestion of vegetables irrigated with this water. This paper studies the presence of 41 trace elements plus nitrate and bromate in groundwater, using a multivariate statistical tool based on Principal Component Analysis and a geostatistical Kriging method to map the results. Principal Component Analysis revealed 11 significant principal components, which account for 82% and 81% of the total variance (information) respectively for the two dates analysed. Ordinary Kriging was applied to draw maps of the trace elements and PC scores. This research breaks new ground in terms of the large number of parameters used and in terms of the analysis of spatiotemporal variations in these parameters. The results obtained indicate that PC1 represents the natural quality of the aquifer (geogenic) and that there is little change in the average PC1 value between the two dates studied (June near the peak recharge point and November at the end of summer). Agriculture is the human activity that causes the greatest variations in the quality of the groundwater due to the use of fertilizers and due to watering crops with wastewater (PC7_J and PC5_N, June and November, respectively). Other elements of industrial origin, which are dangerous for human health, such as Pb, Cu and Cd, are grouped together in other principal components. The results show that the decline, or even complete absence, of natural recharge during the summer months leads to an increase in the TEs produced by human activity. This indicates that a temporary reduction in the natural recharge could worsen the quality of water resources. Based on the interpretation of the estimated maps, a synthetic map was created to show the spatial distribution of the areas affected by geogenic and anthropogenic factors. Studies with a global approach like this one are necessary in that the possible sources of pollution that could alter the quality of the groundwater and the amount of trace elements and other potentially harmful substances could increase as time goes by. The main advantage of the methodology proposed here is that it reduces the number of parameters, so simplifying the results. This makes it easier to interpret the results and manage the quality of the water.

1. Introduction

The increasing development of industrial, agricultural, and residential activities is causing a progressive deterioration in the natural quality of aquifers. Many of the trace elements (TEs) detected in groundwaters have been classified as toxic agents that are dangerous for human health (Boente et al., 2017; Camacho et al., 2011; Goovaerts, 2017; Keshavarzi et al., 2012; Odukoya and Ifarajinm, 2021; Rattan et al., 2005) as they enter the food chain through the consumption of drinking water or agricultural products (Luque-Espinar and Chica-Olmo, 2020; Luque-Espinar et al., 2015; Pekey et al., 2004; Rattan et al., 2005). These pollution processes, which are often slow and involve many different TEs, can have serious impacts on the groundwaters. It is therefore important to investigate the origin, spatial distribution, and

* Corresponding author.
E-mail addresses: ja.luque@csic.es (J.A. Luque-Espinar), mlopez@ugr.es (M. López-Chicano), e.pardo.iguzquiza@csic.es (E. Pardo-Igúzquiza), mchica@ugr.es (M. Chica-Olmo).

https://doi.org/10.1016/j.jenvman.2024.120442
Received 8 November 2023; Received in revised form 26 January 2024; Accepted 20 February 2024
Available online 4 March 2024

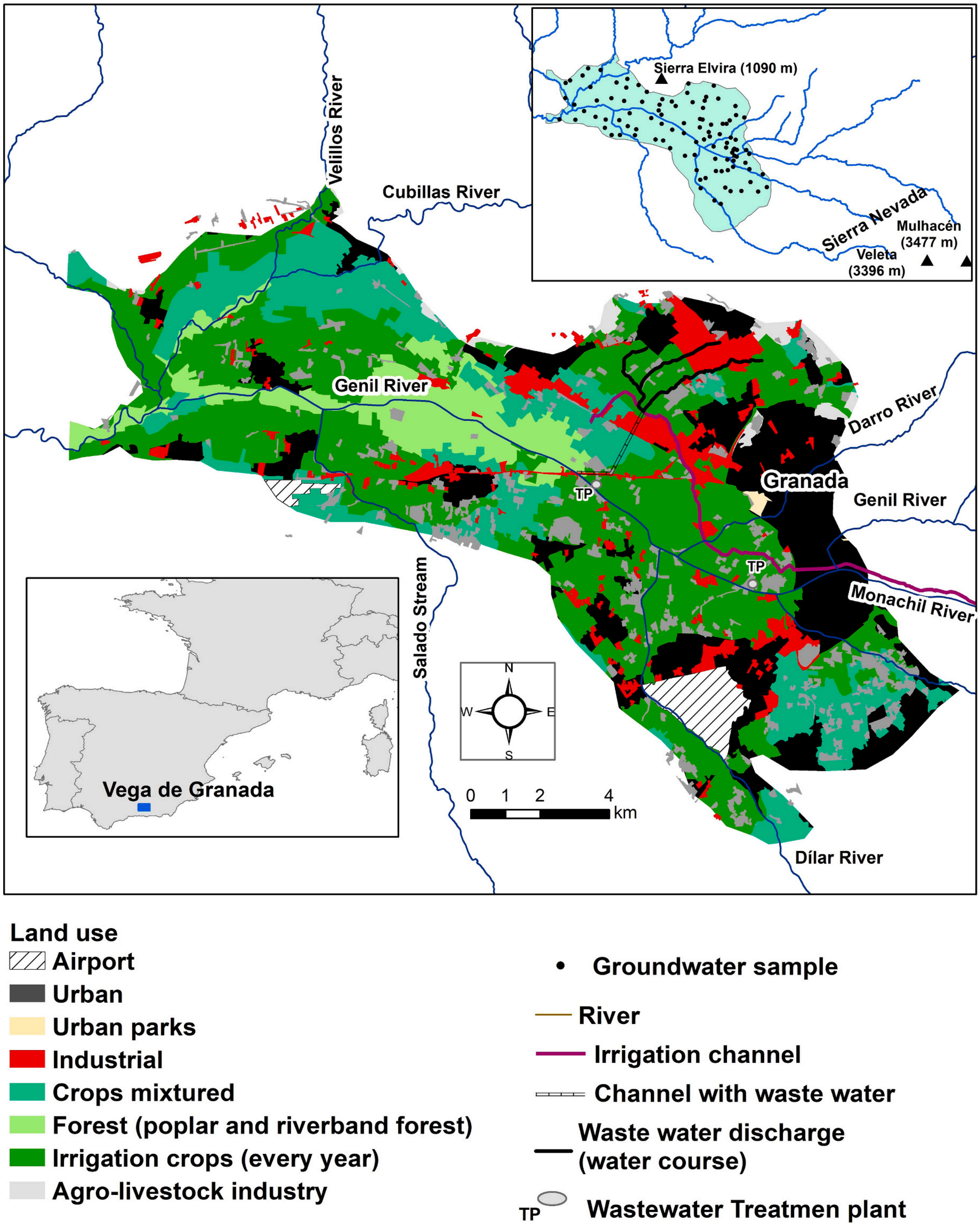

Fig. 1. Location of the VGA: sampling points and land uses.

relationships between the different TEs in these water bodies, in that multiple exposures to these elements, even in low concentrations, can cause serious health problems (Islam et al., 2014; Xiao et al., 2014; WHO, 2019).

The pollution of groundwater, in particular by trace elements, is a cause of great concern in many countries. Despite this, most research on this question has focused either on very few trace elements or on certain very specific aspects (Xiao et al., 2019; Lu et al., 2022). Some studies focus on just one TE, often As (Huq et al., 2020). However, very few articles offer an overall approach to the analysis of the environmental problems affecting groundwater.

Multivariate statistical approaches are powerful tools for environmental studies, among other reasons, because they offer a better understanding of the results of water analysis, and can identify the different sources of pollution that most influence the system being studied. They also help reveal hidden relationships between variables while reducing large chemical datasets to a small number of factors with minimal information loss (Banerjee et al., 2016; Chen et al., 2007; Busico et al., 2018; Dang et al., 2021; Hou et al., 2017; Khound and Bhattacharyya, 2016; Pant et al., 2020; Wu et al., 2019; Zhang et al., 2015).

Geostatistics is another powerful tool for the spatial analysis of data and solving problems relating to estimation and simulation of hydrogeological spatial variables, in general, and groundwater quality, in particular (Chilès and Delfiner, 1999; Goovaerts, 1997). It has been successfully applied to solve a range of different hydrogeological problems (Baalousha, 2010; Brindha et al., 2020; Goovaerts, 2019; Hossain and Patra, 2020).

This research studies groundwater from a detrital aquifer located in an area with high anthropogenic activity for which a sufficient density of samples was available. In any investigation of water quality, it is essential to try to identify possible sources of pollution. To this end, a specific methodology was developed for the analysis of the data that allowed us to link the spatial distribution of the TEs with their sources (Chica-Olmo et al., 2014; Rodriguez-Galiano et al., 2018; Luque-Espinar and Chica-Olmo, 2020).

The following 41 TEs were studied: Ag, As, Au, Ba, Be, Bi, Cd, Co, Cr, Cs, Cu, Ga, Ge, Hf, Hg, In, Ir, Li, Mn, Mo, Nb, Ni, Pb, Rb, Re, Sb, Sc, Se, Sn, Sr, Ta, Te, Th, Ti, Tl, U, V, W, Y, Zn, and Zr. The nitrates (NO_3) and bromates (BrO_3^-) present in the groundwater samples were algo analysed, because they are both potentially harmful compounds of anthropic origin. The groundwater samples were taken at two dates in the annual hydrological cycle, at the end of the period of maximum recharge (beginning of June, 96 samples) and at the end of summer (beginning of November, 104 samples).

A large amount of information was gathered and then analysed using PCA, SPSS statistical software, and the geostatistical Kriging method. SGeMS geostatistical software was used to display the distribution of the parameters and PC_scores on an estimation grid. The final maps were then prepared with ArcGIS 10.5.

The objective of this study was to analyse the spatial distribution of the TEs and the PC_scores within the aquifer and any changes in these parameters over time, and to identify their possible origins or sources of pollution. No rain was recorded during the study period (June–November).

2. Materials and methods

2.1. Study area and sampling

The study was conducted in the Vega de Granada aquifer (VGA) is SE Spain, in an area where different geological materials outcrop. These include Paleozoic metamorphic materials in Sierra Nevada and Mesozoic carbonated materials in Sierra Elvira, together with the deposits of quaternary detrital materials that form the aquifer (IGME, 2020) (Fig. 1). From a geochemical point of view, the metamorphic materials have higher values for most of the TEs than those observed in the sedimentary materials in the Basin of Granada, where the aquifer is located (Luque-Espinar et al., 2018).

The aquifer has a multilayer sedimentary structure with alternating grain sizes. These include conglomerates, sands, clays, and silts (Luque-Espinar et al., 2008). The natural recharge of the aquifer occurs mainly due to the surface runoff from the surrounding Sierra Nevada mountains in the form of rainfall and melted ice and snow. Large amounts come from direct recharge from the rain that falls on top of the aquifer (surface area 200 km^2), estimated at about 10 hm^3/year. Other less important inputs include the lateral underground inflows into the aquifer from outcrops of evaporitic rocks located to the south (near the airport) and from the carbonate aquifer of Sierra Elvira to the north, which has hot springs waters. These inputs show high concentrations in some TEs. The groundwater flows mainly east-west with a piezometric level that varies between 100 m and 2 m in depth, depending on the direction of the flow.

The groundwater shows mainly magnesium sulphate and calcium bicarbonate facies (García Soldado, 2009). Important parameters such as Ca, Mg, Na, SO_4^{2-}, Cl, F, and electrical conductivity have a similar spatial distribution to the main components found in the samples from June (PC1_J) and November (PC1_N) (Fig. 3b and d). The main source of groundwater pollution is intensive agricultural activity over a large part of the surface above the aquifer, in which nitrogen-based fertilizers are frequently used. The impact of farming on water quality has increased over the last two decades, as demonstrated by various studies (Chica-Olmo et al., 2014; Rodriguez-Galiano et al., 2018). New emerging pollutants, such as ibuprofen, paracetamol, and caffeine, have also been observed (Luque-Espinar et al., 2015; Luque-Espinar and Chica-Olmo, 2020). Other factors contributing to groundwater pollution include leaks from urban drainage systems (in the city of Granada and 26 nearby municipalities), and the use of wastewaters mixed with surface waters for irrigation (Luque-Espinar and Chica-Olmo, 2020; Rodriguez-Galiano et al., 2018). Specific sources of pollution include industrial estates and livestock farms (especially cattle) scattered around the region. A significant part of local industry is devoted to the manufacture of agricultural products. These include olive oil, whose production is concentrated to the northeast and south of the city of Granada.

The concentration of nitrates, a frequent subject of research, could be considered the parameter that best represents the deterioration in the quality of the groundwater in this aquifer. According to Chica-Olmo et al. (2014), in 1980 the average nitrates value was 40 mgr/L, while by 2003 it had risen to 70 mgr/L. The concentration continued to rise and when they conducted their study, readings of over 90 mgr/L were obtained. During the current research, in some sectors where measurements had been taken in previous studies, the concentration was even higher at an average of over 110 mgr/L.

The groundwater was sampled in June and November 2018, at the end of the aquifer recharge period and the end of summer, respectively. 96 samples were collected in June and 104 in November. The samples were collected according to the procedure described in Luque-Espinar et al. (2015), and the chemical analyses were conducted at the Scientific Instrumentation Centre at the University of Granada.

2.2. Methodology

The experimental data were analysed using PCA, together with geostatistical spatial estimation using the Kriging method, performed with SPSS 19 and SGeMS software. The resulting thematic maps were created with ArcGIS 10.5. These methods are frequently used in the spatial analysis of data in environmental pollution studies (Boente et al., 2017; Kim et al., 2019; Kumar et al., 2017; Joseph et al., 2019; Liao et al., 2018; Magesh et al., 2017; Raj Pant et al., 2020).

To facilitate the analysis of experimental data, the dimensions of the multivariate space were reduced by applying the PCA method. This method minimizes the redundancy that occurs when there are high linear correlations between the variables in the database, as happens with some of the parameters studied here. The first stage involved converting the experimental variables into normalized variables, with a mean of 0 and a variance of 1, in order to avoid scaling factors that could affect the magnitude of the variable values. The goodness of fit of the experimental data obtained of both dates by application of the PCA method was also checked. Similar values were obtained for both dates in the KMO test (0.72 and 0.69) and in Bartlett's test of sphericity (4864 and 4753, with a significance p-value of <0.01). This indicates that the database was suitable for the application of PCA.

The principal components were extracted by applying the eigenvalue >1 criterion and a Varimax rotation of the factorial axes in order to simplify the interpretation of the factors (components). For each sampling date, a set of 11 principal components ($PC_{i=1,11}$) were extracted, which represent very similar values for the overall variance (information) explained by the PCA models, 82% (June) and 81% (November). No parameters were eliminated from the analysis and the communality values (proportion of variance of the variable explained by the PCA model) were high in most cases (near 1), and were never less than 0.5.

Finally, the Ordinary Kriging method (OK) was applied to spatially

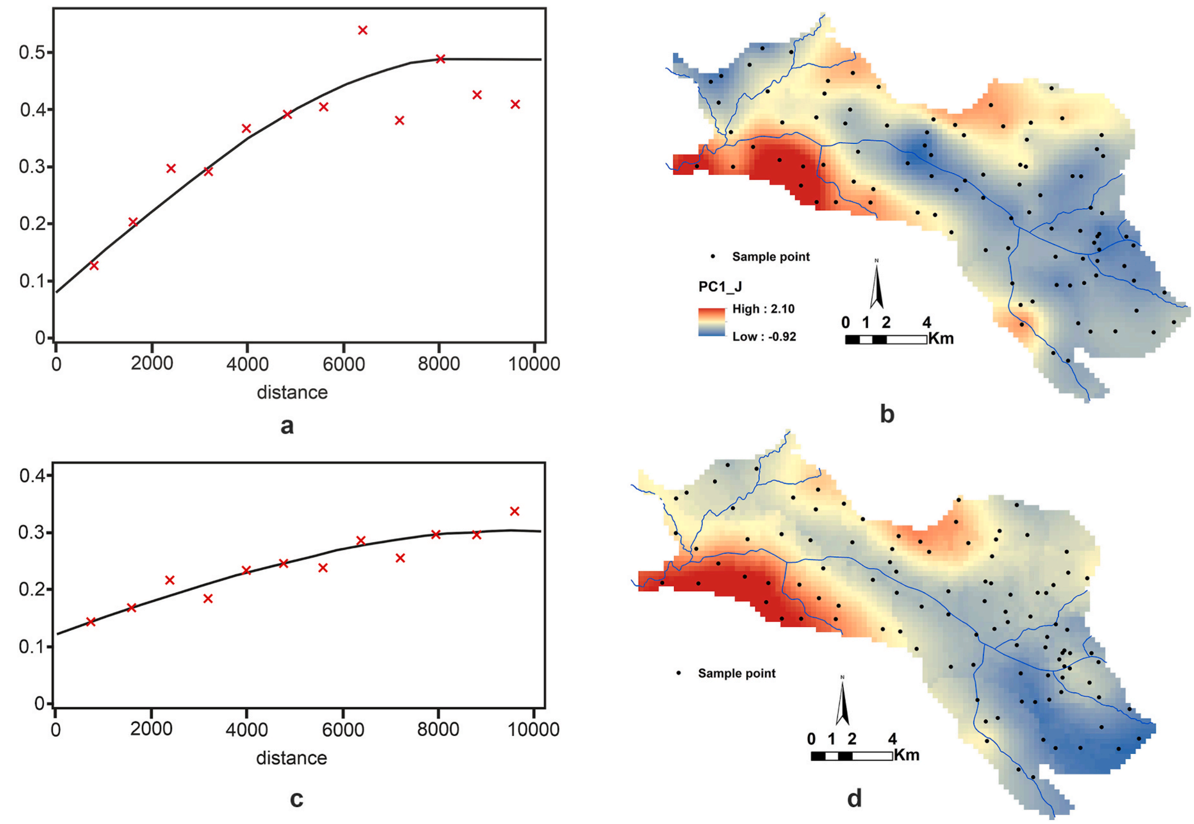

Fig. 2. a–d. Variograms and estimated maps for PC1_scores for June and November.

estimate both the experimental variables and the PC_i_scores, which synthesize the information obtained from the variables. The analysis of the estimated maps facilitated our interpretation of the spatial distribution of the different anthropic sources of pollution. As part of the geostatistical analysis, the experimental variograms of the parameters and PC_scores were calculated and interpreted. It was observed that the first PC_i (PC1) is better spatially structured (variogram) than the last (PC11). This may be related to the fact that the first PC_i provides a larger information load (eigenvalue). In all cases, experimental variograms were fitted to the spherical models and validated using a cross-validation method. Indicator Kriging (IK) was used to map the probability $P[PC_i(x) > pc]$ from the estimate of the indicator variable: $I\_PC_i = 1$ if $PC_i(x) > pc$ and 0 if not, where pc is a reference cutt-off value (third quartile Q_3). The interpretation of the results was synthesized on a map that shows the areas most influenced by water of geogenic origin (saline waters affected by geothermal activity, water affected by evaporitic rocks and waters from the main recharge water from Sierra Nevada) and water affected by anthropic activities (urban, industrial and agricultural).

3. Results

3.1. Experimental data

SM_Table 1 presents the mean, maximum, and minimum values for the experimental data for the two sampling dates, as well as the frequency of non-detected values, and in some cases, the reference values established in the guidelines of the World Health Organization (WHO, 2019) or in Spanish law.

For the set of parameters studied (TEs), no clear trends were observed in terms of an increase or decline in the mean concentration values over the period from June to November, although in general the increases in concentrations were greater than the decreases. Concentrations increased in 44% of the parameters by an average of 60%, while in the remaining 56% of the parameters, they fell by an average of 41%. In the scatter diagram of the mean concentration values for the two dates (SM_Fig. 2A logarithmic scale) the points are situated around the slope line 1. This indicates that water quality remained homogeneous over the study period (with a high coefficient of correlation $R2 = 0.90$). These general trends in the aquifer are largely due to the hydrodynamic processes that take place within it and the natural quality of the groundwater recharge. However, relatively large differences (%) were observed in the concentration of some trace elements (SM_Fig. 2B), probably due to anthropogenic pollution of the aquifer. Significant increases in concentration were noted in the following elements: Zn, Pb, Cu, Mn, Ga, Tl, W, Tl, as well as in BrO3- and NO3-. In some of these parameters, the mean value increased by over 100% (SM_Fig. 2B). This increase can be linked to anthropogenic activities, particularly agriculture and industry, as well as to the use of wastewater in irrigation and the fact that the aquifer is not recharged during the hot dry summer period. The concentration of some elements fell, including Te, Se, Bi, Th, Hf, Au, Cr, Va, and In. This was probably due to the lack of surface runoff recharge from the surrounding mountains (Sierra Nevada).

Within the group of 43 parameters studied, the number of elements that were "not detected" (nd) was slightly higher in June than in November. This may be due to the dilution of these elements during the period of aquifer recharge, which typically ends around June.

The TEs studied here are potentially prejudicial for the environment and for public health and in many cases exceeded the values indicated in WHO guidelines (2019). For instance, Mn showed values of over 100 μg/L in June and November, far exceeding the maximum limit permitted by WHO guidelines (50 μg/L). These high readings were mainly found in sectors affected by evaporitic materials and hot springs. In areas affected by urban land uses and irrigation with wastewaters, values of between 50 and 100 μg/L were observed. The maximum values for November were slightly higher than those observed in June.

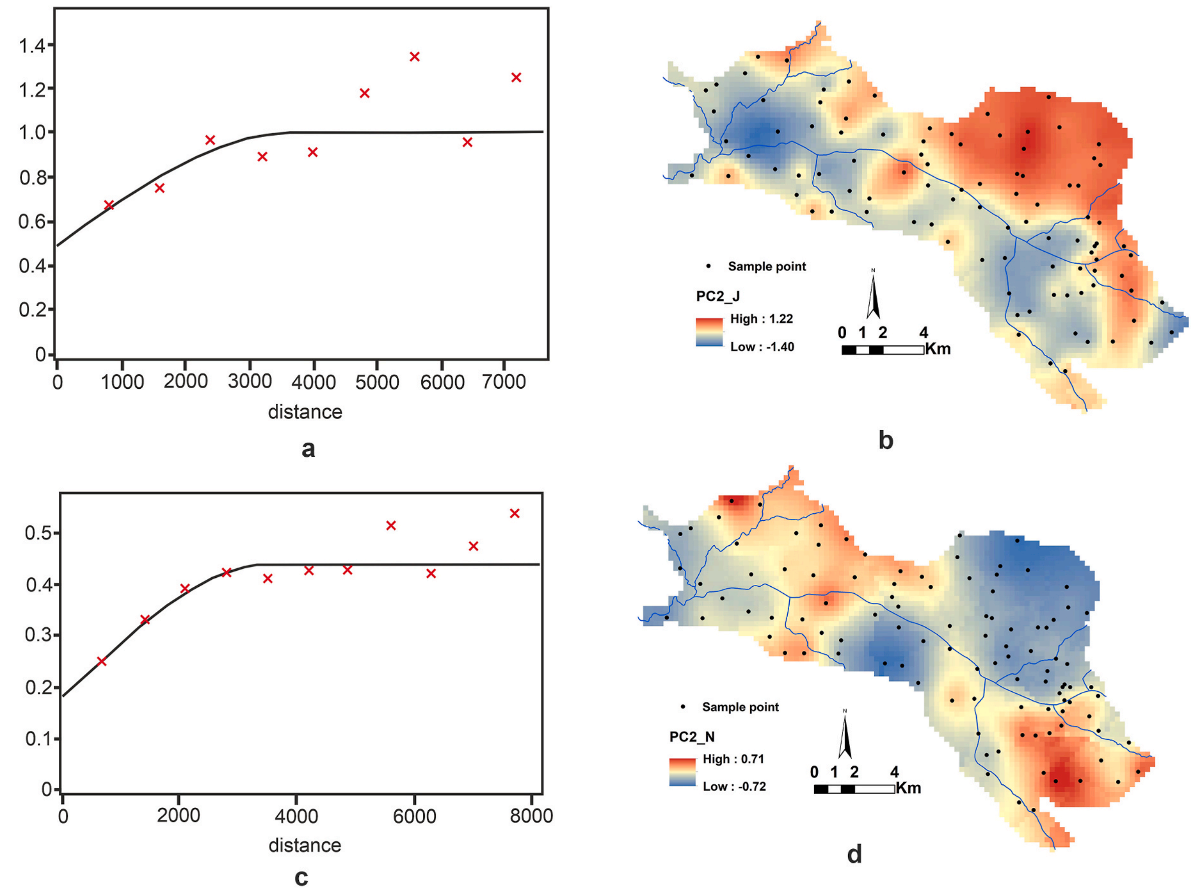

Fig. 3. a–d. Variograms and estimated maps for PC2_scores for June and November.

A significant number of samples (27% in June and 74% in November) had NO3- concentrations of over 50 mg/L (WHO, 2019). The maximum values were often observed in the western part where agriculture is more intensive and the piezometric level is closer to the surface. Maximum values for November were often twice as high as those for June.

Although the WHO guideline for Hg (6 μg/L) was not exceeded, various samples exceeded the limit established in Spanish law (1 μg/L). There were three times as many such samples in June as in November. In addition, Hg concentrations were higher in the samples taken in June than in those taken in November, especially in areas affected by urban land use and irrigation with wastewater.

The (WHO, 2019) guideline for Se (40 μg/L) was not exceeded anywhere. However, 11 samples taken in November exceeded the limit established in Spanish law (10 μg/L), and several others had concentrations that were very close to the limit. All these samples were taken in urban areas, although a few were also influenced by evaporitic materials. None of the samples taken in June exceeded these limits, although the highest value was clearly related with evaporitic materials.

The (WHO, 2019) guideline for Ni (70 μg/L) was not exceeded anywhere. However, eight of the June samples and one from November exceeded the limit established in Spanish law (20 μg/L). The concentrations were twice as high in June as in November. While the Ni levels in June were more affected by anthropic factors than by natural ones, the highest values in November were due to the effects of evaporites.

The guideline for As (10 μg/L) was not exceeded, although concentrations of over 5 μg/L were recorded at several points. Concentrations were higher in June than in November. The highest values observed in June were related with irrigation with wastewater and to a lesser extent, with hot spring waters. However, in November, the highest As concentrations were detected in the area influenced by hot spring waters.

The guideline for BrO3- (10 mg/L) was not exceeded anywhere, although there was a clear difference between the concentrations in June and November. The values for June were well below 1 mg/L, while in November higher concentrations, close to the guide figure, were observed. At both sampling times, the highest values were closely associated with urban uses and agricultural areas irrigated with wastewater.

The guideline for Cr was not exceeded either (50 μg/L), although there are some points with values that were very close to the limit. As in other cases, the concentrations for June were higher than those for November. In general, there were few points with high concentrations and these were due to human activity.

The guideline level for U (30 μg/L) was reached at the same sampling point in both June and November. On both occasions, the highest concentration values for this element were due to the presence of evaporitic materials and do not seem to have been influenced by human activities.

3.2. Spatial principal components analysis

The matrices for factorial loads, or components, rotated from June and November are included in SM_Table $2_{A\text{-}B}$. In order to facilitate interpretation of the results, the values for the interval [−0.3 - 0.3] interval have been removed because they represent low weights of PC_i in the communality of the variable explained by the PCA model. The values for the components are mostly positive, with the odd exception in the samples from June, where Ga and Ba have slightly negative values of −0.52 in PC1_J, and Te has a value of −0.71 in PC2_J.

The first two components have similar information loads (eigenvalues of the correlation matrix) in the two sample groups. In June, PC1_J and PC2_J explained 26% and 16% of total variance, with an accumulated value of 41%, and in November PC1_N and PC2_N

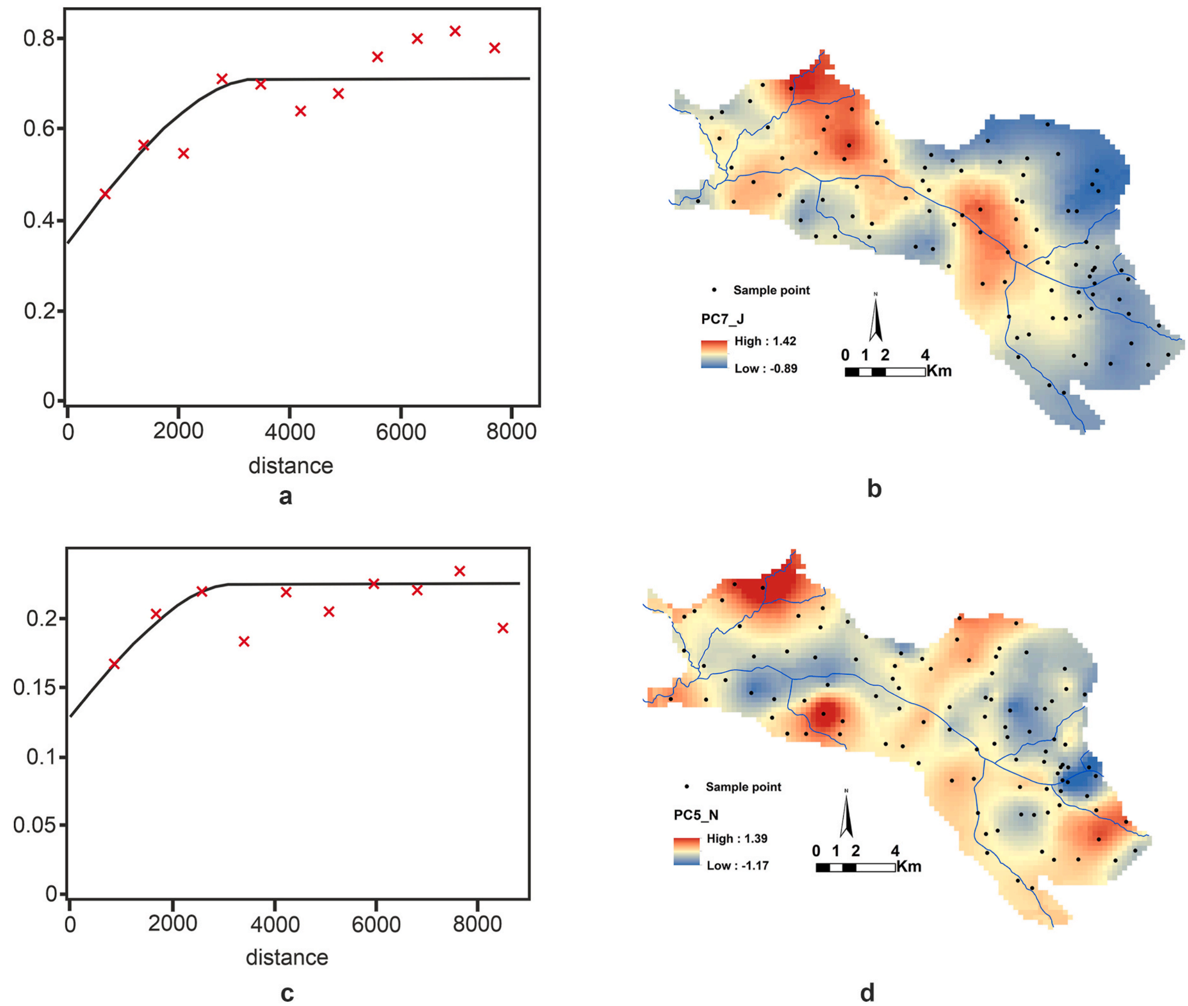

Fig. 4. a–d. Variograms and estimated maps for PC7_J (a,b) and PC5_N (c,d).

explained 25% and 11% of the variance, with an accumulated value of 36%. The rest of the components have eigenvalues of less than 10% at both dates. As can be seen in the scatter diagram showing the values of the factorial loads for the first component PC1_J and PC1_N (SM_Fig. 2), there is a very clear linear tendency, with a relatively high value of the coefficient of correlation for linear regression, $R^2 = 0.70$. This clear linear relationship was also observed in the comparison of the average values for the TEs (Fig. 2A). Re, U, Mo, Li, Ni, Co, Sr, Ge, Ga and Ba had slightly higher values in June, while Re, U, Mo, Hf, Li, Ge, Ni, Th, Ti and Sr were above average in November. PC1 is related above all with the average natural quality of the aquifer recharge water.

PC2 has a smaller information load than PC1, with 16% and 11% in June and November, respectively. A few elements with a high factorial load (correlation) in PC2, such as Ir, Nb and Ta, appeared in both June and November, although on the whole there was no obvious correspondence between the two dates. Ag, In, Nb, Sn, Te, Ge, Ta, Ir and Tl stood out in June and Ir, Nb, W, Bi, Hg, Ta and Zr in November. PC2 is considered to be related above all with anthropic activity (industrial and urban), and with the changes observed in the study period due to the important drop in natural groundwater recharge over the summer months.

The rest of the components have eigenvalues of less than 10% in June and November with a number of elements with significant factorial load, which in general gets progressively lower. These components may be related with different types of land use, which can give rise to isolated local pollution processes, so altering the natural quality of the water in the aquifer. They may also be due to the presence of evaporitic geological materials and hot springs waters (Sierra Elvira area, Fig. 1). Components PC7_J and PC5_N, with high values of NO_3^- and BrO_3^- in the component matrix, could also be highlighted as indicators of agriculture-based pollution processes and irrigation with wastewaters. These phenomena are particularly evident in the western part of the aquifer. PC8_J and PC10_N are also of interest for the environment in that they are also related with pollution, in this case by heavy metals such as Cu, Cd and Pb.

The PCA model enabled us to calculate the factorial scores (PC_i_-scores) at the sampling points for their geostatistical analysis and spatial interpretation using estimated maps. These synthetic variables are obtained as a linear combination of the experimental variables weighted by the factorial coefficients matrix. From the geostatistical point of view, the PC_i_score variograms for the first components are better structured than those for the las components, in both Juen and November, and have greater scopes and lower nugget effects. This is because the PC_i have different information loads (eigenvalues), and these are far greater in the first components than in the others. The experimental variograms for these variables were adjusted to spherical models to enable us to draw up estimation maps by kriging. These maps are interesting because they provide a multivariate viewpoint of the interpretation of the spatial distribution of the TEs studied in the aquifer and their relationship with the different sources of pollution.

The PC1_scores show clear spatial regionalization within the aquifer. The variograms are spatially well-structured, in both June and November, with substantial ranges in the order of 7–8 km and relatively low nugget effects (Fig. 2a and c). The estimated maps produced by

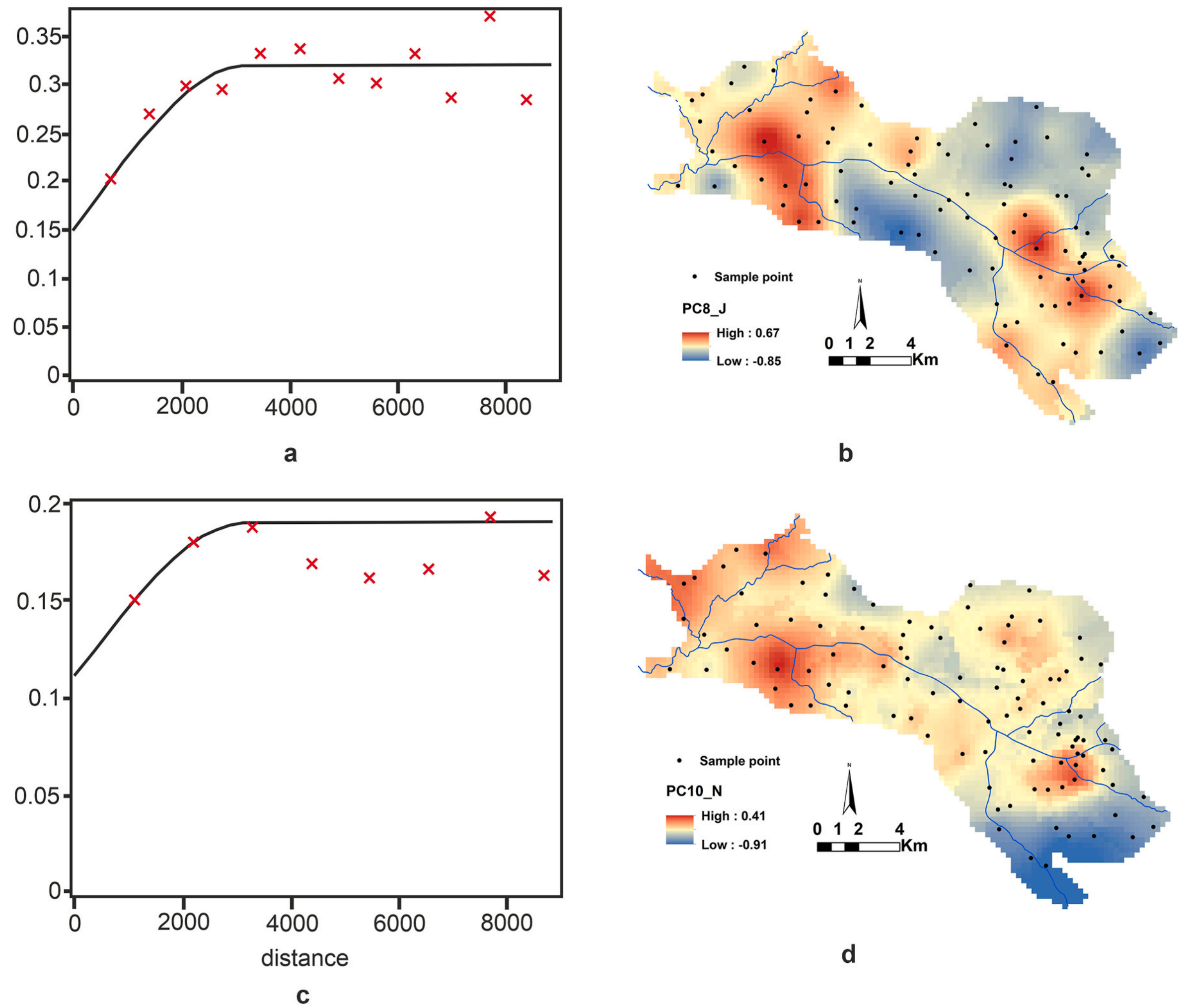

Fig. 5. a–d. Variograms and estimated maps of PC8_J and PC10_N.

kriging clearly highlight the main areas of recharge of the aquifer with low PC1 values in the eastern and central parts coinciding with the route of the main river (Genil) and its subsidiaries. The high PC1 values are preferentially situated in the southwest, coinciding with the areas with a high presence of evaporitic materials; and in the northern edge coinciding with the presence of underground hot water (Sierra Elvira).

The estimated maps for PC1_scores have similar spatial distribution characteristics to the maps for the TEs with the greatest load in PC1, at both sampling dates (SM_Table 1). For example, SM_Fig. 3a–d shows the estimated maps for Re, an element with a high factorial load in June (0.89) and November (0.93). Both the adjusted variograms and the estimated maps are very similar for the two sampling dates (SM_Fig. 1a–d). These maps also closely resemble the estimated maps for the PC1_scores.

The variograms for the PC2_scores (Fig. 3a–d) show a spatial structuring that is slightly worse than PC1. This is only to be expected given that PC2 represents a smaller % of total variance and is related with aspects of the distribution of the most local TEs. The variograms have ranges of around 3–4 km, in both June and November. The nugget effect is slightly greater, a fact that reflects an increase in the random component compared to that observed in PC1.

The PC2_score for June highlights the areas most affected by anthropic activity, mainly industrial and urban areas (Fig. 3b). The high values are located in sectors with a high concentration of urban (e.g. the city of Granada wastewaters) and industrial activities and, in a more specific way, the area near the airport. In November, the high values are situated around the main area of recharge of the aquifer and in areas influenced by hot spring and evaporitic waters (Fig. 3d).

The kriging maps for the other PC_i_scores highlight more or less confined areas with a significant weight of the TEs related with these components. These areas are related with sources of pollution linked to wastewater discharge from industrial, urban and agricultural land uses. PC7_J and PC5_N can be highlighted due to their direct relationship with agricultural activity, with high values in the components matrix for NO_3^- and BrO_3^-, indicators of agricultural pollution processes and irrigation with wastewaters, which are especially important in the western sector. The variograms have ranges of between 3 and 4 km and nugget effects of around 50% of overall variability (Fig. 4a–d).

PC8_J and PC10_N are worth highlighting for their environmental interest. These components are related with industrial pollution processes involving the heavy metals Cu, Cd and Pb. In a similar way to the previous case, it was observed that the variograms have a range of a few kilometres and the nugget effects exceed 50% of overall variance (Fig. 5a–d).

The other PCs define isolated, localized sectors with high concentrations of the elements with the greatest factorial load, linked to wastewaters and industrial, urban and agricultural land uses.

The IK method was applied to obtain spatial probability maps of PC_i_scores. An example of IK results corresponding to PC1 is shown in Fig. 6. As can be seen, the indicator variables for the two dates have well-aligned with similar variogram models. The estimated probability maps clearly show the division of the study area into three areas influenced by

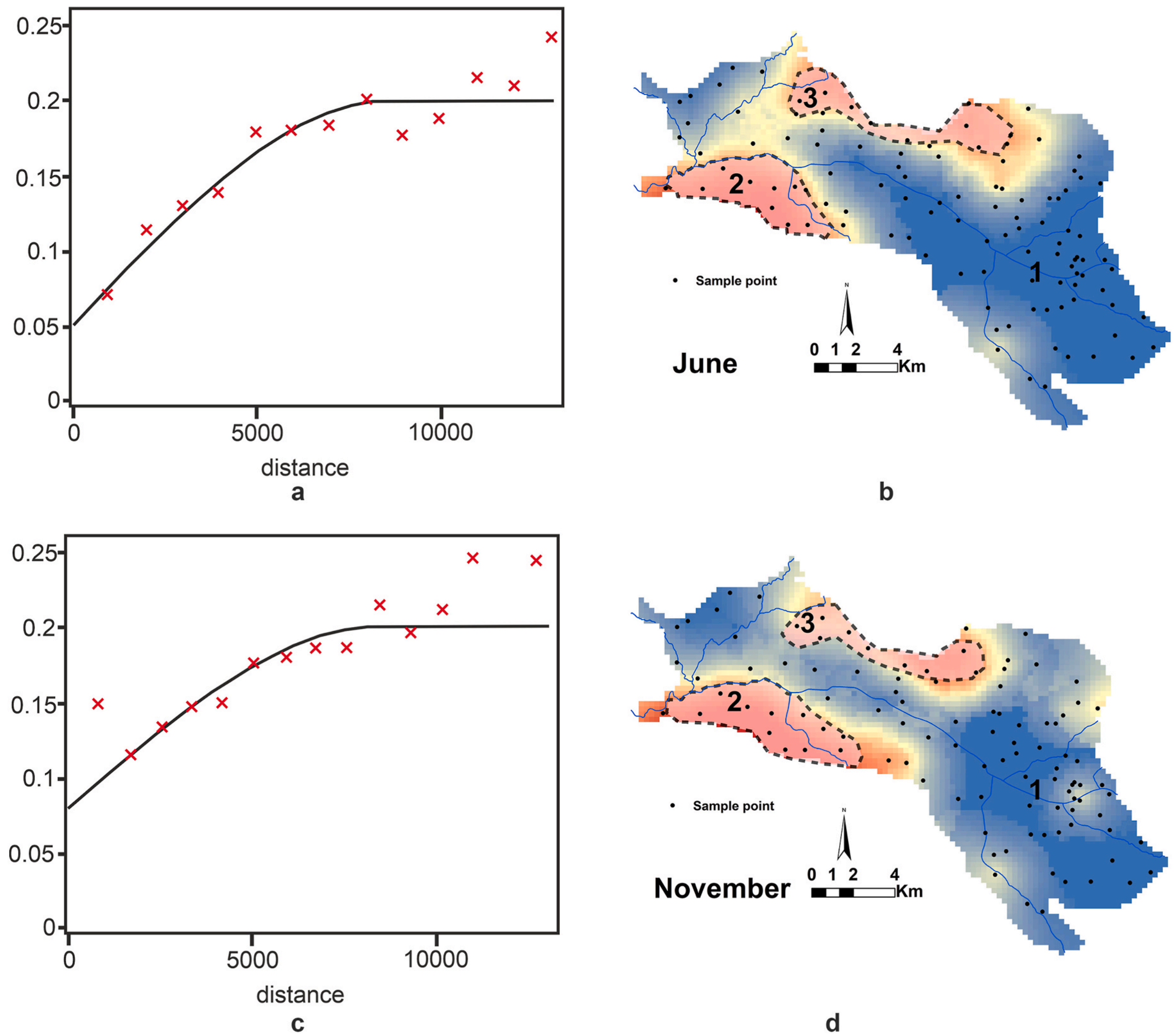

Fig. 6. a–d. Variograms of indicator variables of the two dates (a and c). Estimations of indicator variables (b and d). 1) main zone of natural groundwater recharge from surface runoff and precipitation, 2) zone influenced by evaporitic materials and 3) area influenced by thermal water.

geogenic factors (using Q_3 as the cut-off value): 1) the main area of natural groundwater recharge from surface runoff and precipitation; 2) the area influenced by evaporitic materials; 3) the area influenced by hot spring water.

3.3. *Spatial analysis of the temporal differences between November and June*

The next stage was to study the differences between November and June in the concentration of significant elements and in the synthetic variables (PC_i_scores). The experimental variograms showed that the differences are spatially regionalised within the aquifer. The variograms were fitted with spherical models for the creation of the kriging maps. The analysis of the maps revealed the areas in which the greatest changes (increase or decrease) in these variables take place over the period June–November. It also enables us to relate them to the different sources of pollution and land use.

As an example, Fig. 7a and b shows the variogram and the estimated map for the difference in the concentration of Re, an element that is representative of water quality. In absolute terms, the differences in concentration are quite small in the aquifer as a whole. Large parts of the aquifer have negative values, except in urban areas (the city of Granada and its surrounding area) and more specific local areas where waste-waters are used for irrigation, in which small increases in concentration can be observed. As a whole, there is little change in the natural quality of the aquifer between the two dates, as manifested by the behaviour of this TEs.

As regards the differences in the PC_i_scores, the most notable is the difference [PC1_N-PC1_J], related with the change over time in the average natural quality of the aquifer. This variable has a well-structured variogram, adjusted with a spherical model with a range of 4 km and a nugget effect of slightly less than 50% of the overall variance (Fig. 7c). The estimated map (Fig. 7d) sets out the areas in which the greatest changes have taken place. These are, above all, areas of intensive agricultural and urban activity, and to a lesser extent industrial use. These areas tend to coincide with those in which there are relatively small variations in natural quality.

The change over time in dangerous heavy metals, Pb, Cu, and Cd, was assessed from the perspective of the kriging maps of the difference between the two sampling dates [PC10_N-PC8_J]. The greatest increases over the period June to November took place in areas with industrial land use and also in urban areas and sectors in which there are waste-water discharges (Fig. 7e and f).

3.4. *Spatial distribution map of the influence of geogenic and anthropogenic factors on groundwater quality*

A detailed interpretative analysis was conducted of the set of results

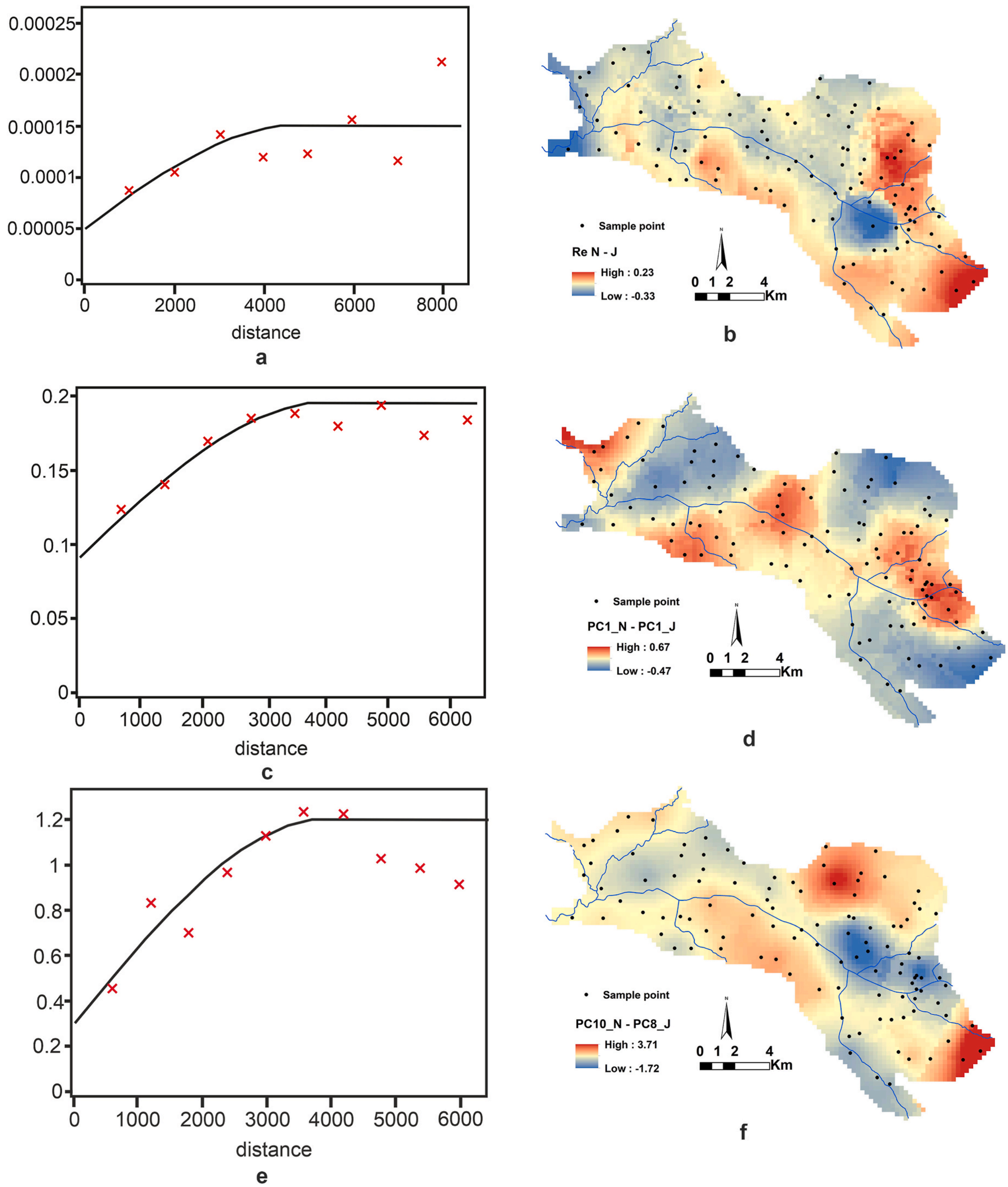

Fig. 7. a–fVariograms and estimated maps of the temporal differences: Concentration of Re (a, b). Difference [PC1_N-PC1_J] (c, d). Difference [PC10_N-PC8_J] (e, f).

obtained for the two dates. This enabled us to draw up a synthesis map highlighting the influence of geogenic and anthropogenic pollution on groundwater in the aquifer (Fig. 8). Seven thematic classes were established: agriculture, urban, industrial, mixed, evaporites, hot springs and recharge. The “mixed” category was included to cover those cases in which it was impossible to distiguish any more specific influence. However, the most significant factor is likely to be irrigation with wastewater.

The map shows that the eastern half of aquifer was more influenced by industrial and urban uses, while agriculture was dominant factor in the west. It also indentifies areas influenced by industrial and urban activities and areas affected by irrigation with wastewater. The urban activities of the city of Granada extend their influence westwards through the most permeable part of the aquifer situated below the Genil River. Lastly, the sector affected by natural recharge is relatively small due to the widespread impact of anthropic activities.

4. General discussion

Pollution of both anthropogenic and geogenic origin is a common problem in many detritic aquifers in different countries and has therefore been the subject of extensive research. However, most of the studies consulted offer a quite specific, limited view of the problem of trace element pollution and rarely analyse the two sources of pollution together (Huq et al., 2020; Hussain et al., 2008; Kourgialas et al., 2017; Mendieta-Mendoza et al., 2023).

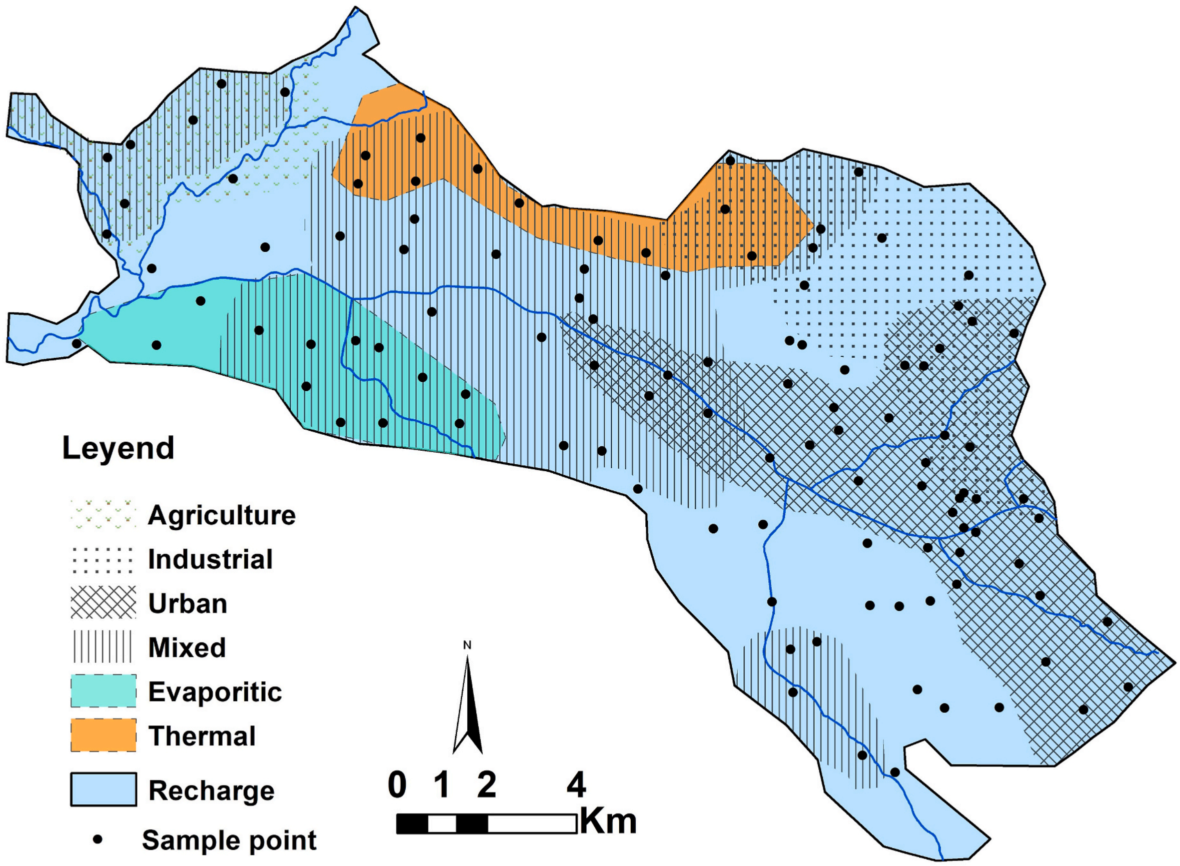

Fig. 8. Mapping of geogenic and anthropogenic influence on groundwater quality.

The studies that try to differentiate between the different sources of trace elements tend to focus on just a few elements. For example, Blake et al. (2017) presented a procedure to determine whether uranium discovered in groundwater was of anthropogenic or geogenic origin for which they applied multiparametric, hydrogeochemical and isotopic techniques.

The most complete analysis of this type was made by Busico et al. (2018). Using multivariant statistical analyses they differentiated between the anthropogenic and geogenic origin of a group of the most abundant ions and 12 trace elements for a particular date. The hydrogeological context for this study was relatively simple and just one category of anthropogenic influence was identified, while the remaining categories were geogenic. However, these authors did not analyse this question over time nor did they use geostatistical tools to estimate the factors.

Bearing in mind the state of the art of research in this field, this article makes a substantial contribution in terms of the methodology for analysing detritic aquifers that are subject to complex influences of natural and anthropogenic origin. It also analyses their behaviour over time and the influence of the recharge. As a result, it was possible to differentiate between the different sources of geogenic and anthropogenic pollution. However, in order to understand the influence of these sources more precisely and thereby improve the management of water resources and the control of anthropogenic pollution, the following tasks must be performed:

a) Analysis of nitrogen isotopes. This parameter enables us to differentiate between urban and agricultural sources of pollution.
b) Complete analysis of the chemical composition of wastewaters.
c) Composition of the fertilizers used by local farmers. These products are probably the most important source of pollution in many detritic aquifers. In addition to nitrates, they can also be a source of chlorine, sodium, calcium, magnesium, ammonium, phosphates and various different trace elements.
d) Find out more detailed information about the irrigation of agricultural land in the area, i.e. when and where irrigation takes place, the origin of the water and the amount involved. A full hydrochemical analysis would also have to be conducted.

5. Conclusions

This case study shows the current situation of the quality of the groundwater in the VGA, from the perspective of the concentration of a wide set of TEs.

The quality of the groundwater in the VGA is affected by three main factors:

- The quality of the recharge water.
- The effects of evaporitic rocks and hot spring water.
- Anthropic activity (agricultural and industrial activity and urban land use).

The method applied here, based on geostatistical and multivariant statistical methods (PCA), has proved effective for the analysis of the spatiotemporal data gathered during this research. The kriging maps facilitated the interpretation of the spatial distribution of the variables and their relationship with different sources of pollution as well as the changes in these variables over time.

Six types of influence (agricultural, industrial, urban, saline, hot springs, and recharge) on the chemical quality of groundwater have been observed. In some sectors these influences overlapped and additional categories such as agricultural-wastewater, industrial-urban and mixed influences were identified. Although, in general terms, the average quality of the water in the aquifer is quite similar in June (end of the recharge period) and November (end of the summer).

The anthropic activity that most influences the natural quality of the groundwater is agriculture (fertilizers and irrigation with wastewater).

The Río Genil, the main river in this area, has a clear influence on the chemistry of the groundwater, and serves as a boundary between saline and hot spring waters. It also spreads urban pollution.

Perhaps the greatest weakness of this research is that no clear differentiation was achieved between the nitrates from wastewaters and those from nitrate-based fertilizers. This problem could be overcome with an analysis of the nitrogen isotopes.

CRediT authorship contribution statement

Juan Antonio Luque-Espinar: Conceptualization, Data curation, Formal analysis, Supervision, Validation, Writing – original draft, Writing – review & editing, Methodology. **Manuel López-Chicano:** Formal analysis, Writing – original draft. **Eulogio Pardo-Igúzquiza:** Conceptualization, Methodology, Writing – original draft. **Mario Chica-Olmo:** Conceptualization, Methodology, Writing – original draft, Writing – review & editing, Funding acquisition.

Declaration of competing interest

The authors declare that they have no known competing financial interests or personal relationships that could have appeared to influence the work reported in this paper.

Data availability

Data will be made available on request.

Acknowledgements

This research has been supported by Research Group RNM-122 of the Junta de Andalucía (Spain).

Appendix A. Supplementary data

Supplementary data associated with this article can be found, in the online version, at https://doi.org/10.1016/j.jenvman.2024.120442.

Principal abbreviations used

TEs	Trace Elements
PCA	Principal Components Analysis
VGA	Vega de Granada Aquifer
PC_i	Principal Component scores
IK	Indicator Kriging
OK	Ordinary Kriging

References

Baalousha, H., 2010. Assessment of a groundwater quality monitoring network using vulnerability mapping and geostatistics: a case study from Heretaunga Plains, New Zealand. Agric. Water Manag. 97, 240–246.

Banerjee, S., Kumar, A., Maiti, S.K., Chowdhury, A., 2016. Seasonal variation in heavy metal contaminations in water and sediments of Jamshedpur stretch of Subarnarekha river, India. Environ. Earth Sci. 75 (3), 1–12.

Blake, J.B., Harte, P., Becher, K., 2017. Differentiating anthropogenic and natural sources of uranium by geochemical fingerprinting of groundwater at the Homestake uranium mill, Milan, New Mexico, USA. Environ. Earth Sci. 78, 384. https://doi.org/10.1007/s12665-019-8385-y.

Boente, C., Matanzas, N., García-González, N., Rodríguez-Valdés, E., Gallego, J.R., 2017. Trace elements of concern affecting urban agriculture in industrialized areas: a multivariate approach. Chemosphere 183, 546–556.

Brindha, K., Paul, R., Walter, J., Leong Tan, M., Singh, M.K., 2020. Trace metals contamination in groundwater and implications on human health: comprehensive assessment using hydrogeochemical and geostatistical methods. Environ. Geochem. Health 42, 3819–3839.

Busico, G., Cuoco, E., Kazakis, N., Colombani, N., Mastrocicco, M., Tedesco, D., Voudouris, K., 2018. Multivariate statistical analysis to characterize/discriminate between anthropogenic and geogenic trace elements occurrence in the Campania Plain. Southern Italy. Environ. Pollut. 234, 260–269.

Camacho, L.M., Gutiérrez, M., Alarcón-Herrera, M.T., Villalba, M., Deng, S., 2011. Occurrence and treatment of arsenic in groundwater and soil in northern Mexico and southwestern USA. Chemosphere 83, 211–225.

Chen, K., Jiao, J., Huang, J., Huang, R., 2007. Multivariate statistical evaluation of trace elements in groundwater in a coastal area in Shenzhen, China. Environ. Pollut. 147, 771–780.

Chica-Olmo, M., Luque-Espinar, J.A., Rodriguez-Galiano, V., Pardo-Igúzquiza, E., Chica-Rivas, L., 2014. Categorical indicator kriging for assessing the risk of groundwater nitrate pollution: the case of Vega de Granada aquifer (SE Spain). Sci. Total Environ. 470–471, 229–239. https://doi.org/10.1016/j.scitotenv.2013.09.077.

Chilès, J.P., Delfiner, P., 1999. Geostatistics: Modeling Spatial Uncertainty. Wiley, Toronto, p. 720.

Dang, P., Gu, X., Lin, C.Y., Xin, M., Zhang, H., Ouyang, W., Liu, X.T., He, M.C., Wang, B. D., 2021. Distribution, sources, and ecological risks of potentially toxic elements in the Laizhou Bay, Bohai Sea: under the long-term impact of the Yellow River input. J. Hazard Mater. 413, 125429 https://doi.org/10.1016/j.jhazmat.2021.125429.

García-Soldado, M.J., 2009. Metodología basada en SIG para el Desarrollo de un Sistema Soporte de Decisión en la gestión de la calidad de los recursos hídrico de la Vega de Granada. Universidad de Granada, Phd Thesis, p. 352.

Goovaerts, P., 1997. Geostatistics for Natural Resources Evaluation. Oxford University Press, New York, p. 477.

Goovaerts, P., 2017. The drinking water contamination crisis in Flint: modelling temporal trends of lead level since returning to Detroit water system. Sci. Total Environ. 581–582, 66–79. https://doi.org/10.1016/j.scitotenv.2016.09.207.

Goovaerts, P., 2019. Geostatistical prediction of water lead levels in Flint, Michigan: a multivariate approach. Sci. Total Environ. 647, 1294–1304. https://doi.org/10.1016/j.scitotenv.2018.07.459.

Hossain, M., Patra, P.K., 2020. Contamination zoning and health risk assessment of trace elements in groundwater through geostatistical modelling. Ecotoxicol. Environ. Saf. 189, 110038 https://doi.org/10.1016/j.ecoenv.2019.110038.

Hou, D., O'Connor, D., Nathanail, P., Tian, L., Ma, Y., 2017. Integrated GIS and multivariate statistical analysis for regional scale assessment of heavy metal soil contamination: a critical review. Environ. Pollut. 231 (1), 1188–1200. https://doi.org/10.1016/j.envpol.2017.07.021.

Huq, M.E., Fahad, S., Shao, Z., Sarven, M.S., Khan, I.A., Alam, M., Saeed, M., Ullah, H., Adnan, M., Saud, S., Cheng, Q., Ali, S., Wahid, F., Zamin, M., Raza, M.A., Saeed, B., Riaz, M., Khan, W.U., 2020. Arsenic in a groundwater environment in Bangladesh: occurrence and mobilization. J. Environ. Manage. 262, 110318 https://doi.org/10.1016/j.jenvman.2020.110318.

Hussain, M., Ahmed, S.M., Abderrahman, W., 2008. Cluster analysis and quality assessment of logged water at an irrigation project, eastern Saudi Arabia. J. Environ. Manange. 86, 297–307.

IGME. 2020, http://info.igme.es/visorweb/(check 16IV2021).

Islam, M.S., Han, S., Ahmed, M.K., Masunaga, S., 2014. Assessment of trace metal contamination in water and sediment of some rivers in Bangladesh. J. Water Environ. Technol. 12 (2), 109–121.

Joseph, P., Nandan, S.B., Adarsh, K.J., Anu, P.R., Varghese, R., Sreelekshmi, S., Preethy, C.M., Jayachandran, P.R., Joseph, K.J., 2019. Heavy metal contamination in representative surface sediments of mangrove habitats of Cochin. Southern India. Environ Earth Sci 78, 490. https://doi.org/10.1007/s1266 5-019-8499-2.

Keshavarzi, B., Moore, F., Najmeddin, A., Rahmani, F., 2012. The role of selenium and selected trace elements in the etiology of esophageal cancer in high risk Golestan province of Iran. Sci. Total Environ. 433, 89–97. https://doi.org/10.1016/j.scitotenv.2012.04.033.

Khound, N.J., Bhattacharyya, K.G., 2016. Multivariate statistical evaluation of heavy metals in the surface water sources of Jia Bharali river basin, North Brahmaputra plain, India. Appl. Water Sci. 1–10. https://doi.org/10.1007/s13201-016-0453-9.

Kim, H.R., Yub, S., Oh, J., Kim, K.H., Leec, J.H., Moniruzzaman, M., Kime, H.K., Yuna, S. T., 2019. Nitrate contamination and subsequent hydrogeochemical processes of shallow groundwater in agro-livestock farming districts in South Korea. Agric. Ecosyst. Environ. 273, 50–61. https://doi.org/10.1016/j.agee.2018.12.010.

Kourgialas, N.N., Karatzas, G.K., Koubouris, G.C., 2017. A GIS policy approach for assessing the effect of fertilizers on the quality of drinking and irrigation water and wellhead protection zones (Crete, Greece). J. Environ. Manange. 189, 150–159. https://doi.org/10.1016/j.jenvman.2016.12.038.

Kumar, M., Ramanathan, AL., Tripathi, R., Farswan, S., Kumar, D., Bhattacharya, P., 2017. A study of trace element contamination using multivariate statistical techniques and health risk assessment in groundwater of Chhaprola Industrial Area, Gautam Buddha Nagar, Uttar Pradesh, India. Chemosphere 166, 135–145. https://doi.org/10.1016/j.chemosphere.2016.09.086.

Liao, F., Wang, G., Shi, Z., Huang, X., Xu, F., Xu, Q., Guo, L., 2018. Distributions, sources, and species of heavy metals/trace elements in Shallow groundwater around the Poyang Lake, East China. Exposure Health 10, 211–227. https://doi.org/10.1007/s12403-017-0256-8.

Lu, T.T., Peng, H., Yao, F., Ferrer, A., N, S., Xiong, S., Niu, G., Wu, Z., 2022. Trace elements in public drinking water in Chinese cities: insights from their health risks and mineral nutrition assessments. J. Environ. Manage. 318, 115540 https://doi.org/10.1016/j.jenvman.2022.115540.

Luque-Espinar, J.A., Chica-Olmo, M., 2020. Impacts of anthropogenic activities on groundwater quality in a detritic aquifer in SE Spain. Exposure Health 12, 681–698. https://doi.org/10.1007/s12403-019-00327-7.

Luque-Espinar, J.A., Chica-Olmo, M., Pardo-Igúzquiza, E., García-Soldado, M.J., 2008. Influence of climatological cycles on hydraulic heads across a Spanish aquifer. J. Hydrol 354, 33–52. https://doi.org/10.1016/J.JHYDROL.2008.02.014.
Luque-Espinar, J.A., Navas, N., Chica-Olmo, M., Cantero-Malagón, S., Chica-Rivas, L., 2015. Seasonal occurrence and distribution of a group of ECs in the water resources of Granada city metropolitan areas (SE Spain): pollution of raw drinking water. J Hydrol 531 (3), 612–625. https://doi.org/10.1016/j.jhydrol.2015.10.066.
Magesh, N.S., Chandrasekar, N., Elango, L., 2017. Trace element concentrations in the groundwater of the Tamiraparani river basin, South India: insights from human health risk and multivariate statistical techniques. Chemosphere 185, 468–479. https://doi.org/10.1016/j.chemosphere.2017.07.044.
Mendieta-Mendoza, A., Renteria-Villalobos, M., Randall, H., Ruíz-Gomez, S., Ríos-Lopez, M., 2023. Chemical degradation of agricultural soil under arid conditions by the accumulation of potentially toxic elements and salts. Geoderma regional, e00736. https://doi.org/10.1016/j.geodrs.2023.e00736.
Odukoya, A.M., Ifarajinm, W.T., 2021. Assessment of selected major and trace elements in groundwater of Lagos based on land use and implication on human health. Appl. Water Sci. 11, 54. https://doi.org/10.1007/s13201-021-01383-8.
Pant, R.R., Zhang, F., Rehman, F.U., Koirala, M., Rijal, K., Maskey, R., 2020. Spatiotemporal characterization of dissolved trace elements in the Gandaki river, central Himalaya Nepal. J. Hazard Mater. 389, 121913.
Pekey, H., Karakaş, D., Bakoglu, M., 2004. Source apportionment of trace metals in surface waters of a polluted stream using multivariate statistical analyses. Mar. Pollut. Bull. 49 (9–10), 809–818.
Rattan, R.K., Datta, S.P., Chhonkar, P.K., Suribabu, K., Singh, A.K., 2005. Long-term impact of irrigation with sewage effluents on heavy metal content in soils, crops and groundwater—a case study. Agric. Ecosyst. Environ. 109, 310–322. https://doi.org/10.1016/j.agee.2005.02.025.
Rodriguez-Galiano, V.F., Luque-Espinar, J.A., Chica-Olmo, M., Mendes, M.P., 2018. Feature selection approaches for predictive modelling of ground water nitrate pollution: an evaluation of filters, embedded and wrapper methods. Sci. Total Environ. 624, 661–672. https://doi.org/10.1016/j.scitotenv.2017.12.152.
WHO, 2019. Drinking-water. World Health Organization fact sheets. https://www.who.int/news-room/fact-sheets/detail/drinking-water. (Accessed 24 March 2020).
Wu, J., Li, P., Wang, D., Ren, X., Wei, M., 2019. Statistical and multivariate statistical techniques to trace the sources and affecting factors of groundwater pollution in a rapidly growing city on the Chinese Loess Plateau. Hum. Ecol. Risk Assess. https://doi.org/10.1080/10807, 039.2019.15941–56.
Xiao, J., Jin, Z., Wang, J., 2014. Geochemistry of trace elements and water quality assessment of natural water within the Tarim River Basin in the extreme arid region, NW China. J. Geochem. Explor. 136 (1), 118–126.
Xiao, J., Wang, L., Deng, L., Jin, Z., 2019. Characteristics, sources, water quality and health risk assessment of trace elements in river water and well water in the Chinese Loess Plateau. Sci. Total Environ. https://doi.org/10.1016/j.scitotenv.2018.09.322, 2004 – 2012.
Zhang, Z., Abuduwaili, J., Jiang, F., 2015. Heavy metal contamination, sources, and pollution assessment of surface water in the Tianshan Mountains of China. Environ. Monit. Assess. 187 (2), 1–13.